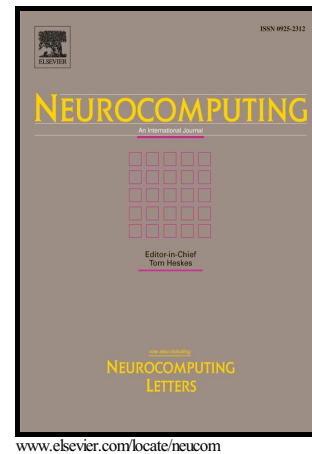# Author's Accepted Manuscript

Detection of Brain Tumor in 3D MRI Images using Local Binary Patterns and Histogram Orientation Gradient

Solmaz Abbasi, Farshad Tajeripour

# Detection of Brain Tumor in 3D MRI Images using Local Binary Patterns and Histogram Orientation Gradient

Solmaz Abbasi, Farshad Tajeripour

School of Electrical and Computer Engineering Shiraz University, Shiraz, Iran

Solmaz.abbasigharghani@gmail.com
tajeri@shirazu.ac.ir

## Abstract

Brain tumor pathology is one of the most common mortality issues considered as an essential priority for health care societies. Accurate diagnosis of the type of disorder is crucial to make a plan for remedy that can minimize the deadly results. The main purpose of segmentation and detection is to make distinction between different regions of the brain. Besides accuracy, these techniques should be implemented quickly.

In this paper an automatic method for brain tumor detection in 3D images has been proposed. In the first step, the bias field correction and histogram matching are used for pre-processing of the images. In the next step, the region of interest is identified and separated from the background of the Flair image. Local binary pattern in three orthogonal planes (LBP-TOP) and histogram of orientation gradients (HOG-TOP) are used as the learning features. Since 3D images are used in this research we use the idea of in local binary pattern in three orthogonal planes in order to extend histogram orientation gradients for 3D images. The random forest is then used to segment tumorous regions. We evaluate the performance of our algorithm on glioma images from BRATS 2013. Our experimental results and analyses indicate that our proposed framework is superior in detecting brain tumors in comparison with other techniques.

## 1. Introduction

Nowadays with the accelerating developments in science and technology and availability of medicinal data there is a need for more accurate machine learning algorithms. In recent decades, many researchers focus on processing medical data using machine learning algorithms [1,2].

Brain tumor is a growth of abnormal cells inside the brain [3]. A tumor threat depends on a combination of different factors such as type of the tumor, location, size of the tumor, and the way the tumor is spread and developed. Glioma is the most common primary brain tumor in adults. They arise from glial cells and they can be classified into four grades; grade 3 or 4 is the high-grade glioma. Grades 1 and 2 can be used as low-grade glioma tumors in treated group [4].

Magnetic resonance imaging is a medical imaging technique used by radiologists to study the anatomy of the body. As MRI can present a lot of information about the soft tissue of the human body anatomy, these images can also contribute to the diagnosis of the brain tumor [5,6]. These images are also used to analyze and study the behavior of the brain. In this imaging technique, it is also possible to make different tissue contrast making it a useful tool for imaging different desirable structures. Regarding the nature and appearance of the brain tumors, just one MRI technique is not enough for segmentation of the brain tumor including all area. Nowadays a combination of different MRI techniques is usually used to diagnose tumor. These techniques include $T_1$ weighted MRI, $T_1$ weighted MRI with contrast enhancement $(T_{1c})$, $T_2$ weighted MRI, and $T_2$ weighted MRI with fluid-attenuated inversion recovery $(T_{2Flair})$ [7]. In $T_1$ Weighted MRI images with contrast enhancement (i.e. $T_{1c}$), the tumor borders look brighter because of the accumulation of contrast agent in brain vessels. MRI contrast agent are a group of contrast media that are used to improve the visibility of the internal body structure. In $T_{1c}$ images, the Necrotic and active tumor area can be easily recognized. In methods with $T_2$ weighted MRI, the Edema area which has surrounded the tumor looks bright. The $T_2$ Weighted MRI with fluid-attenuated inversion recovery $(T_{2Flair})$ is a special method which helps to separate edema from cerebrospinal fluid (CSF) [7]. In order to have a precise and accurate segmentation of tumor area, a sequence of these MRI images $(T_1, T_{1c}, T_2, T_{2Flair})$ should be used which can be called multi-quality MRI image. Figure 1 presents a case of a patient's tumor with $T_1, T_{1c}, T_2, T_{2Flair}$ MRI images.
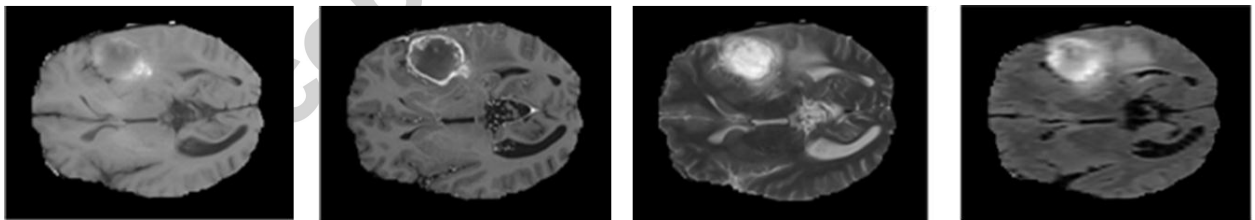


Fig. 1. Typical diagnostic MR scanning modalities, left to right: $T_1, T_{1c}, T_2, T_{2Flair}$

Nowadays with regards to the fact that a lot of data is generated in clinical institutes, image segmentation in a reasonable time is impossible. Moreover the manual analyses of the images are very time-consuming and tiring. Another issue with these techniques is that there is a noticeable variety in labels produced by the experts of different medical specialties [8]. Applying automatic or semi-automatic methods by which the images can be analyzed with computers seems to be more effective and desired. Accomplishing such an automatic process is very challenging due to the large variety in the tumor texture appearance, heterogeneous shape, similarity between tumors and natural texture, and the high irregularity, discontinuity, and

unclear borders of gliomas. The goal of automatic or semi-automatic techniques is to detect the tumor area reliably and accurately since the high speed and high accuracy in texture detection is a very vital in radiotherapy and surgery.

In recent years, different methods of segmentation for the brain tumor images have been proposed. Great advances have been made in the field of differential power analysis and medical image processing. Cai et al. [9] and Verma et al. [10] use the intensity of a large number of the MRI multi-quality images to create the feature vector. Then they use the support vector machines in classifying stage. They not only be able to segment the healthy tissue, but also they can segment the sub-region of the healthy and tumor tissues.

Ruan et al. [11] also detect just one region of the tumor using few numbers of MRI images then they demonstrate that the feature selection improves the results clearly compared to their previous work [12]. Jenson and Schmainda [13] investigate different neutral networks to detect invasive brain tumor using multi-parameter images (diffusion, perfusion). Shuihua Wang et al. [14] extract stationary wavelet transform features. They propose an automatic system based on PSO and ABC for classification phase. Criminisi et al. [15] apply context-aware features along with generative model as an input to determine the sub-region of the tumor using multi-quality of MRI images. They indicate that by using context-aware features, there will be no need for post processing step of the images. Geremia et al. [16] generate the tumor images artificially and they train discriminative regression forest algorithm using different groups of the features. They argue that this approach not only allows them to segment the patient's images, but it can also let them estimate the density of tumor. Hassan Khotanlou et al. [17] used the idea of inherent symmetry of the right and left hemisphere of human brain. Studies indicate that using the brain symmetry idea help faster diagnosis of tumor or edema. However finding the axis symmetry is a challenging issue and in some rare cases, where the tumor coincides with the axis symmetry, the method fails.

In order to detect brain tumors, Remamany et al. [18] apply a maximum fuzzy entropy based approach to magnetic resonance images. This method is based on adaptive thresholding. MR brain images are classified into two membership functions. Optimal parameters of fuzzy MFs are obtained using the modified particle swarm optimization (MPSO) algorithm. In order to obtain optimal fuzzy entropy parameters, the objective function is considered with maximum fuzzy entropy. Mikael Agn et al. [19] propose a generative method for the segmentation of brain tumor images. Their paper employs tumor prior, which models the shape of the tumor core and complete tumor.

Wang et al. [20] have used a fluid vector to specify the contour about the tumor's boundaries in the images by $T_1$ weighting. Sachdeva et al. [21] have proposed content-based brightness intensity and texture patterns to specify the active contour around the tumor in all MRI imaging methods. Hu et al. [22] determine the probability of a tumor or a background using the difference between $T_{1c}$ and $T_1$ images (images before and after contrast). They then use the entire image to specify the (sphere) boundaries of the tumor. Rexilius et al. [23] have used the growing region algorithm to obtain the tumor area. A. Pinto et al. [24] employ the random decision forest

approach. More specifically, they extract gray level, appearance-based, and context-based features and apply the morphological operator at the post-processing step to increase the segmentation accuracy. Reza et al. [25] exploit novel context features for brain tumor image segmentation, including piece-wise triangular prism surface area (PTPSA), multi-fractional Brownian motion (mBm) and Gabor-like textons. Kumar et al. [26] have proposed a method based on texture using the growing region algorithm. In order to analyze texture, their method exploits a hierarchical segmentation algorithm in different directions. Accordingly, anomalies are identified and then the growing region algorithm is applied. Harati et al. [27] have proposed the fuzzy connectedness algorithm, which considers regional features without knowing spatial constraints for connectedness.

Unsupervised classification was first proposed by Schad et al. [28] for the segmentation of brain tumor images. Accordingly, differences and similarities of texture algorithms were analyzed. Phillips et al. [29] exploit the C-means fuzzy classification method and compares this method with an unsupervised k-nearest neighbor classification method to specify the volume of the tumor during treatment. 2D slices of multi-spectral images are used in this study. Menon et al. [30] propose an automatic segmentation method for brain tumor images. This approach is based on Artificial Bee Colony (ABC) and Fuzzy-C Means (FCM) algorithms. This paper first estimates a threshold using the ABC algorithm and then exploits the FCM algorithm for clustering. Clark et al. [29] extend this method by combining it with knowledge-based methods. Fletcher et al. [31] combine the fuzzy unsupervised classification method with knowledge-based methods.

In most algorithms presented so far, the segmentation is performed on multi-quality sequence of MRI images. Few presented methods are semi-automatic which rely on the user interaction. Although the user interactive property of these techniques making them more flexible [7], there is a need for a user.

In many automatic methods the segmentation of brain tumor images is carried out based on the intensity of voxels and the neighborhood information. These methods are flexible and have reliable results. Other categories of methods, which are based on object detection or local limits, are regarded less effective than previous category of techniques. They have less flexibility on different types of tumor and different information.

In this paper we propose an automatic and fast framework which benefits from the advantages of both categories of methods. In other words, our proposed algorithm applies features that are using the intensity of voxels and neighborhood information together with the object detection and local limit approaches. In order to reduce the time and space complexity of the feature extracting phase and to provide more balanced distribution for the training data, we use a clustering algorithm. This clustering algorithm, which is a kind of thresholding algorithm and is called multi-level Otsu [32], uses only the $T_{2Flair}$ images since in these images the tumor regions are brighter than other regions. Multi-level Otsu is a very fast algorithm and it does not need any parameters to be tuned.

The rest of the paper is organized as follows: Section 2 represents our proposed method in detail. Our experimental results are provided in Section 3. Analyses of the results and discussion are provided in Section 4. Finally, Section 5 concludes the paper by a conclusion part and summarizes our findings.

## 2. Materials and Methods

Brain tumor pathology is one of the most common mortality issues considered as an essential priority for health care societies. Thus accurate diagnosis of the type of disorder is very necessary to make a plan for remedy that can minimize the deadly results. Accurate results can be obtained by computer with the help of automatic systems. In medical imaging the image segmentation is used to diagnose the disease and study the tumor growth.

In this paper an automatic technique for brain tumor detection in 3D images is proposed. Figure 2 illustrates the major steps of the segmentation pipeline.

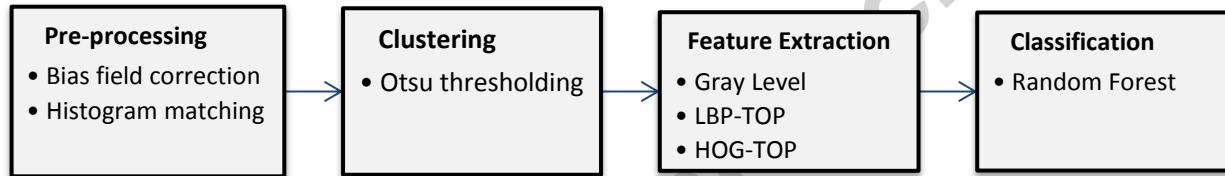| **Pre-processing**<br>• Bias field correction<br>• Histogram matching | → | **Clustering**<br>• Otsu thresholding | → | **Feature Extraction**<br>• Gray Level<br>• LBP-TOP<br>• HOG-TOP | → | **Classification**<br>• Random Forest |

Fig. 2. Illustration of the main blocks used segmentation pipeline.

### 2.1 . Pre-processing

The raw MRI images usually include artifacts such as uneven brightness and additional tissues (e.g. skull, eyes, etc.) which reduce the accuracy of the results. One of the major issues in medical imaging is noise and finding a technique to reduce it. Signal to noise ratio is a measure that compares the level of the desired signal to the level of background noise. Image noise occurs when the signal to noise ratio is relatively low. Noise elimination in the image is a standard method for pre-processing. Diaz et al. [33] investigate different methods for noise removal of brain tumor segmentation. They conclude that these methods reduce the noise in the image; however, they negatively affect the image segmentation in most cases because they destroy the details of the required structures in the image.

Our proposed technique applies "bias field correction" on MRI images using the N4ITK method [34]. N4ITK technique has several small utilities that can be used to reduce such bias field. To estimate the bias field, it uses Legendre polynomials. The evolutionary optimizer searches for the best parameters of a Legendre polynomial (bias field estimate) which minimizes the total energy value of each image after bias field is eliminated [34]. Then, the intensity scale of each sequence was normalized by a histogram matching algorithm implemented in ITK [35]. Histogram matching is a method in image processing of color adjustment of two images using

the image histograms. In this research the histogram of each image is adjusted with the all images mean's histogram.

## 2.2 . Clustering

After pre-processing of the image, the Otsu algorithm is applied to extract the region of interest. This algorithm is unsupervised. As a result, the time and space complexity of the image processing will decrease dramatically. Moreover, this clustering algorithm provides balanced data for training phase. It does not have any parameters to be tuned and consequently it is a fast technique to select the threshold of the image. In order to achieve more accurate clusters this algorithm is applied on each slice of 3D images.

The Otsu algorithm [36] has been applied to the Flair image because in the Flair image, the region of interest is brighter than the other regions (Figure 3). Otsu algorithm is a popular method in image processing and computer vision. This method uses a simple idea which maximizes within-class variance. In this paper the multi-level Otsu algorithm [32] is used for image segmentation.

Considering an image with $L$ gray level $(0, \ldots, L-1)$. $f_i$ is the number of pixels with gray level of $i$; therefor the total pixels equals $N = (f_0 + f_1 + \cdots + f_{L-1})$. In an image the gray-level probability is computed by following equation:

$$p_i = \frac{f_i}{N} \quad , \quad p_i \geq 0 \quad , \quad \sum_{i=0}^{l-1} p_i = 1 \tag{1}$$

If an image is segmented to $k$ clusters, $k-1$ thresholds should be selected. The cumulative probability $w_k$ and mean gray-level $\mu_k$ for each cluster $c_k$ are as follows:

$$w_k = \sum_{i \in c_k} p_i \quad , \quad \mu_k = \sum_{i \in c_k} i.\frac{p_i}{w_k} \tag{2}$$
$$k \in \{0, 1, \ldots, K-1\}$$

Then the mean intensity of the whole image $\mu_T$ and between class variance $\sigma_B^2$ are computed as follows:

$$\mu_T = \sum_{i=0}^{L-1} i.p_i = \sum_{k=0}^{K-1} \mu_k.w_k \tag{3}$$

$$\sigma_B^2 = \sum_{k=0}^{K-1} w_k.(\mu_k - \mu_T)^2 \tag{4}$$

The optimum Thresholds $(t_0^*, t_1^*, \ldots, t_{k-2}^*)$ can be determined by maximizing the between class variance as:

$$\{t_0^*, t_1^*, \dots, t_{k-2}^*\}= \tag{5}$$
$$\text{argmax}_{0 \leq t_0 < \cdots < t_{k-2} < L-1}\{\sigma_B^2(t_0, t_1, \dots, t_{k-2})\}$$
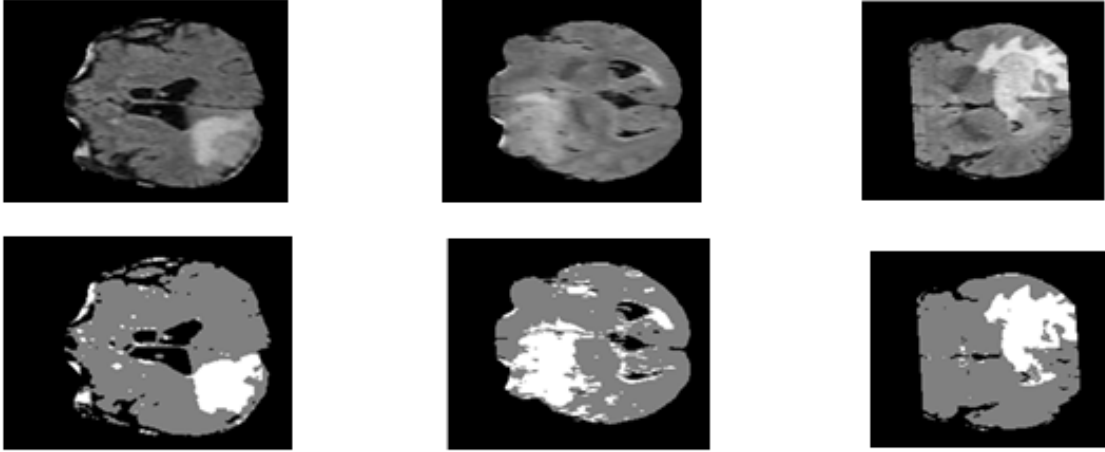


Fig. 3. Separation region of interest from background using OTSU thresholding; First row represents Flair images, second row represents OTSU thresholding.

### 2.3 Feature Extraction

The next step for automatic diagnosis is to extract features from the image. The purpose of extracting features is to make the raw data more usable for the next processing. In this step the features are extracted from different textures in such a way that within-class similarity is maximized and the between-class similarity is minimized. The features used in brain tumor segmentation depend on the type and grade of the tumor because different tumors with different grades can be very different in appearance. Regarding the complexity of different texture structures such as gray material (GM), white material (WM), and Cerebro Spinal Fluid (CSF) in brain images, the feature extraction is a very useful yet challenging task.

One of the most common features used for brain tumor segmentation is the image intensity since there is an assumption that different textures have different gray levels [37]. Because of the existence of noise and heterogeneity, caused by radio frequency couples, using the intensity of the images solely as feature in MRI image segmentation does not produce reliable results.

It seems that using the texture data within the texture features brings about good results for MRI image segmentation because different regions of the tumor have different textural patterns [38–40].

- LBP (Local Binary Patterns)-TOP

The local binary pattern is a simple, quick, and very efficient method for extracting feature from image texture. In this method, first a neighborhood of an image is selected. Then, the intensity of the points existing in this neighborhood is compared with the intensity of the pixel

located in the center of the neighborhood and a binary code is considered for each pixel according to equation 6. In order to make the algorithm rotation-invariant usually circular neighborhood is considered. The pixels whose coordinates are not exactly located on the neighborhood of pixel center are obtained by interpolation [41]. In equation 6, $P$ represents the number of neighborhood pixels of a considered center pixel, $R$ is the neighborhood radius, $g_i$ is the intensity of the neighborhood pixels, and $g_c$ is the intensity of the central pixel.

$$LBP_{P,R} = \sum_{i=0}^{P-1} s(g_i - g_c) 2^i$$

$$s(x) = \begin{cases} 1 & x \geq 0 \\ 0 & x < 0 \end{cases}$$
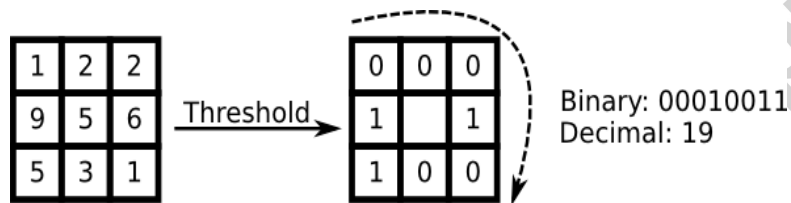
(6)



Fig. 4. Binary code of each pixel in local binary patterns.

A measure called uniformity was proposed in the modified version of LBP [42]. A bit pattern is called uniform if it has at least two circular bit transitions from zero to one or vice versa. For instance, the bit pattern (00000000) has a zero transition and it is uniform; whereas, the bit pattern (01010011) has six transitions and it is not uniform. In the uniform binary pattern mapping, there is a separate output label for each uniform pattern and all non-uniform patterns are assigned to a label. There are two reasons to remove non-uniform binary patterns and assign them to a label. First, it has been shown that most local binary patterns are uniform in natural images. The second reason is that considering uniform patterns instead of all possible patterns provides better detection results. There are signs that indicate uniform binary patterns have more robustness and less sensitivity to noise. In this method, each pixel is labeled by a code of the main texture, which is the best match with local neighbors.

The main LBP operator [43] was only defined with spatial information. Subsequently, it was extended for dynamic textures analysis [44]. One of the methods in dynamic texture analysis considers each voxel in three orthogonal planes (XY-XY-YT). Here, X and Y are spatial coordination and T as the third dimensions represents time. More specifically, binary codes are extracted from all voxels in XY, YT, and XT planes and specified as XY-LBP, YT-LBP, and XT-LBP. Subsequently, histograms are computed and concatenated in a histogram. As we can see in figure 5, each voxel is located at the intersection of the three orthogonal planes (XY, XT, and YT). In these planes, eight neighbors are delineated for each voxel. The local binary pattern for each voxel is separately extracted based on its location on each plane. The final feature vector is achieved by arranging the values of the local binary pattern.
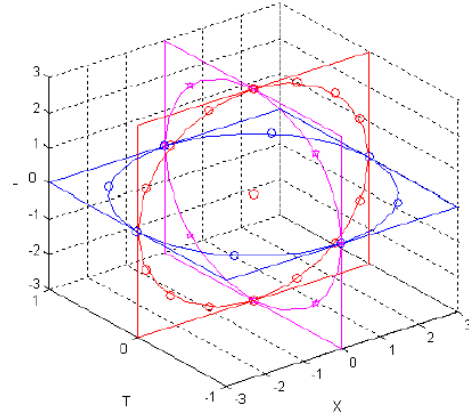
Fig. 5. Neighborhood point of each voxel in three orthogonal plane.

Figure 6 part (a) presents a slice of the initial 3D MRI image with $T_1$ weighting. The uniform local binary pattern algorithm is applied to three orthogonal planes on the entire image. Parts (b), (c), and, (d) are slices of output images considering neighborhood in planes XY, XY, YT, respectively. The feature vector is obtained by concatenating these values together. As we can see, the local binary pattern algorithm has been successful in recognizing edges, flat regions, and the texture structure.
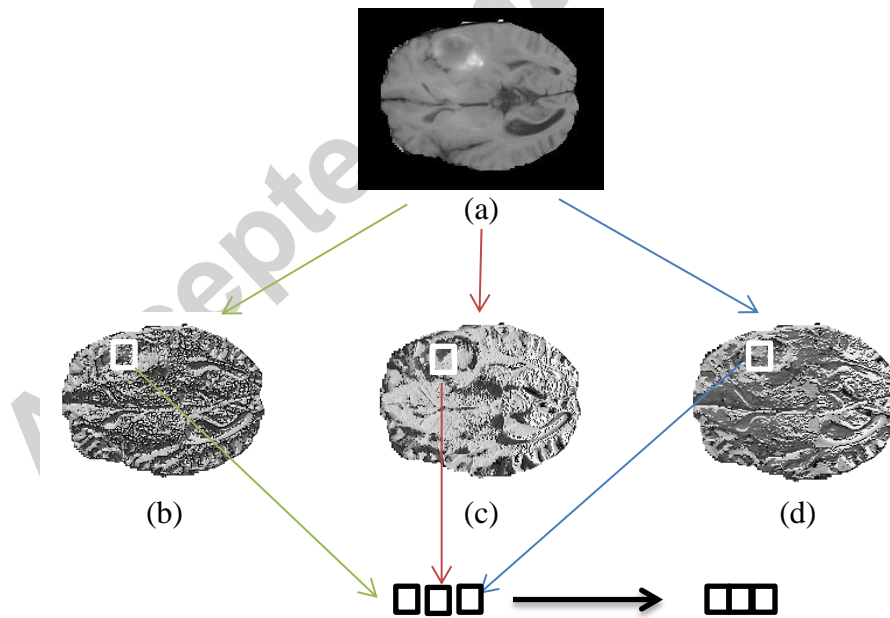


Fig. 6. (a) MRI-T1, (b) LBP-XY plane, (c) LBP-XT plane, (d) LBP-YT plane.

- HOG (Histogram Orientation Gradient)-TOP

Histogram of oriented gradients is a method in computer vision and image processing that is used to detect the object [45]. In this method, the image is divided into small areas that are joined together, they are called cells. The histogram of oriented gradients is extracted from the cells.

First, the image is filtered by Sobel kernel [45] (figure 7) to achieve the image gradient along the $x$ and $y$ directions.

$$[-1 \quad 0 \quad 1] \qquad \begin{bmatrix} -1 \\ 0 \\ 1 \end{bmatrix}$$

Horizontal mask     Vertical mask

Fig. 7. Sobel mask.

$G_x$ , $G_y$ are referred to the image gradient along the $x$ and $y$ directions. Magnitude and angle of the image gradient is calculated at each pixel according to equations 7 and 8. In these equations, $|G|$ is magnitude of gradient, $\theta_g$ is angle of gradient, $i$, and $j$ represent the rows and columns of the image, respectively.To calculate the gradient histogram, angle is divided into $n$ equal distances where $n$ indicates the number of gradient directions or histogram bins. To calculate the histogram, each pixel inside a cell votes to one of the histogram bins based on its gradient angle (Figure 8). These votes are weighed in this pixel based on the gradient size.

$$|G(i,j)| = \sqrt{\left(G_x(i,j)\right)^2 + \left(G_y(i,j)\right)^2} \qquad (7)$$

$$\theta_G(i,j) = tan^{-1}(\frac{G_y(i,j)}{G_x(i,j)}) \qquad (8)$$

After calculating the gradient histogram in each cell, this histogram is allocated to the cell central pixel. Therefore for each pixel an $n$ dimensional vector, which represents its surrounding gradient histogram, is calculated. Dalal and Triggs [46] used $n = 9$ in their research thus for each pixel a vector of length 9 is obtained.
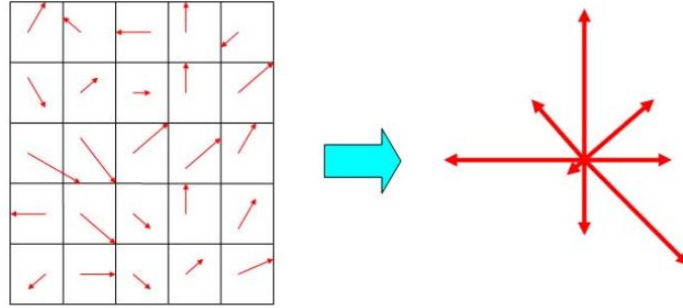
Fig. 8. A cell and histogram orientation gradiant.

The HOG method of feature extraction was proposed for 2D images but in this paper by considering the location of each voxel in the intersection of three orthogonal planes we extend the method to 3D images.

Since 3D images are used in this research we use the idea presented in LBP-TOP [44] in order to extend HOG to 3D images. As it is illustrated in figure 9, for each cell we extract the gradient histogram in XY ,YZ and, XZ planes; therefore we have a vector with the length of $9 \times 3$ for each voxel or cell. Feature extraction step is performed on all MRI modalities.
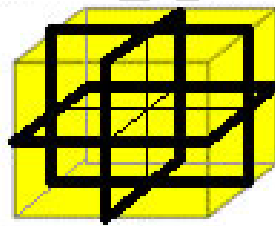


Fig. 9. Cells in three orthogonal plane.

2.4 . Classification

Random Forest [47] are an ensemble learning algorithm for classification, regression, and other tasks that operate by constructing a multitude of decision trees at training time and outputting the class that is the mode of the classes or mean prediction of the individual trees. Random Forest combines Bagging [48] idea and the random selection of features.

In this paper we use Random Forest for classification phase. High accuracy in classification is one of the advantages of this method as it can operate properly with a lot of different inputs.

## 3. Results

Dataset (Brats2013)[1] including $T_1$, $T_2$, $T_{2Flair}$, and $T_1$ with contrast ($T_{1C}$), all were interpolated to 1 mm isotropic resolution. The dataset includes 30 real glioma patients (20 high grade (HG) and 10 low grade (LG)), and 50 simulated glioma patients (25 of each grade). A manual segmentation was also provided distinguishing different labels including: 1) necrosis, 2) edema, 3) non-enhancing tumor, and 4) enhancing tumor, 0) everything else.

Three different categories such as complete tumor, tumor core, and enhanced tumor are considered for the evaluation. The details on these three categories are as follows: Complete Tumor: 1) necrosis, 2) Edema, 3) non-enhancing tumor, 4) enhance tumor; Tumor Core: 3) non-enhance tumor, 4) enhance tumor; and Enhance tumor: 4) enhance tumor).

The region of interest is nearly 20 percent of the entire image which reduces the time. Our proposed method's speed up is related to the feature extraction phase. Since we cluster the input image before training, our method gets speed up. Performing feature extraction on the whole image takes 1516 seconds on average for each image. On the other hand, by performing clustering before feature extraction and getting rid of the unwanted areas in the image, our method takes only 374 seconds on average for feature extraction. Programming language is MATLAB on a computer with an eight core processor (4.0 GHz), and 32 GB of RAM.

As in this paper the feature vector length for each image is 31 (besides the intensity, 3 for local binary pattern and 9×3 for histogram of oriented gradients). The number of base classifiers, decision trees, in Random Forest is set to forty.

We use Dice [49] and Jaccard [50] for evaluation phase and perform ten-fold cross validation for real high grade glioma, leave-one-out scheme for real low grade glioma and two-fold cross validation for synthetic data.

In figure 10, 11 horizontal and vertical axes display patient samples and evaluation criterion respectively. Utilized evaluation criteria are the best evaluation methods for investigation of segmentation accuracy, which their definition is presented in equations 8 and 9. In these equations, $A$ and $B$ indicate grand truth and segmentation result respectively.

$$Dice(A, B) = \frac{2|A \cap B|}{|A| + |B|} \qquad (8)$$

$$Jaccard(A, B) = \frac{|A \cap B|}{|A \cup B|} \qquad (9)$$

Dice Coefficient indicates the overlap between manual segmentation and automatic segmentation. Jaccard Coefficient indicates the similarity of two sets. These values are between 0 and 1 and the higher value indicates more accurate segmentation.

---

[1] http://vsddemo.bfh.ch/WebSite/BRATS/Start2013

Three categories are evaluated for each sample. Therefore, three columns are extracted from each patient in figure 10. For low-grade figure, enhance tumor column is presented only for samples 1, 2, and 8, because data of these samples didn't include enhance tumor class.

In tables 1-4, mean and standard deviation values are calculated. Low standard deviation indicates that the proposed method offers consistent results.

We compared our results with three different researches in [51]. Meier et al. [52] use generative-discriminative hybrid model which generates initial tissue probabilities that are used subsequently for enhancing the classification and spatial regularization. Cordier et al. [53] use Patch-based Segmentation. This segmentation approach is based on similarities between multi-channel patches . Festa et al. [54] use features include MR sequence intensities, neighborhood information, and context information for segmentation.

- BraTumIA software

The result of the proposed method is compared with BraTumIA (Brain Tumor Image Analysis) application. This software can analyze 3D images and analyzing automatic brain tumor images [55]. Oncologists use this software to scrutinize the images accurately. It can segment the tumor including its sub-compartments from MRI of glioma patients. For this, it inputs four different MRI sequences ($T_1$, $T_{1c}$, $T_2$, and $T_{2Flair}$) and outputs volumetric information about the tumor and its sub-compartments (necrotic tissue, active enhancing tumor tissue, non-enhancing tumor tissue, and edema). Also, the software can segment healthy subcortical structures surrounding the tumor. Label maps of the segmented tissues and structures are available as an overlay on the original images.

## 4. Discussion

In table 1 through 3, our results are compared with the algorithms which used Brats2013 dataset. The results indicate that the proposed method has achieved better results in all cases.

In table 4 the results of our proposed method are compared with the acquired results of BraTumIA software. Figure 10, 11 indicate the results of real and synthetic data. One example of each case in real HG and real LG shown in figure 12. Figure 13 indicate 3D representation of data label.

According to the results, in high grade glioma, our proposed method indicates better results in comparison with the results of BraTumIA software. In low grade images this software fails in segmentation.

LBP feature provides the texture information of an image and HOG feature describes local information with gradient histogram. Simply said, the proposed algorithm extracts texture and local information together. The HOG method of feature extraction was proposed for 2D images and in this paper by considering the location of each voxel in the intersection of three orthogonal planes we extend the method to 3D images. Consequently, more neighborhood voxels are considered for each regarding voxel. The shorter length of the feature vector will speed up the

program to run. Using LBP and HOG features together with Random Forest classification algorithm yields significantly better overall results.
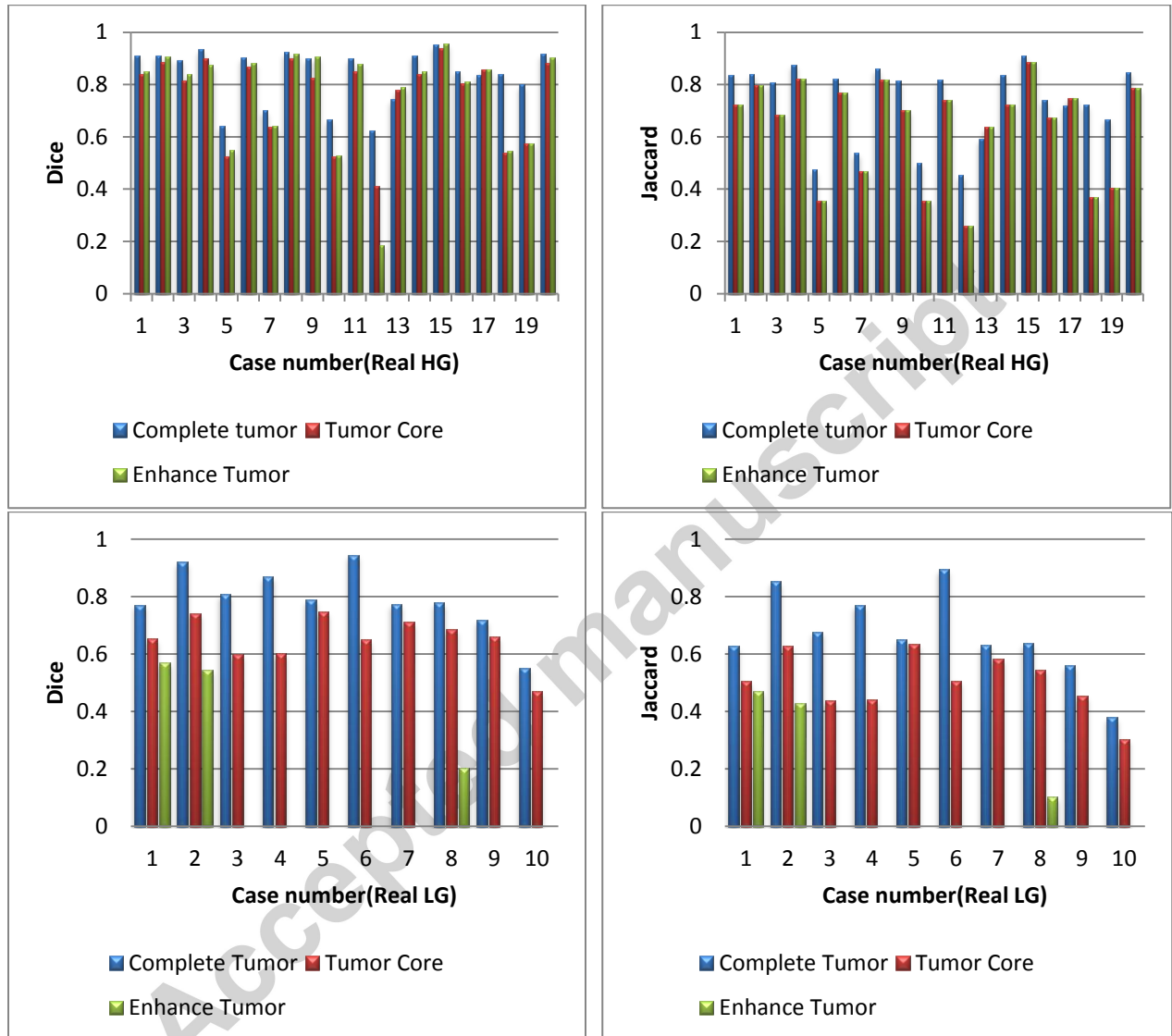


Fig. 10. Evaluation of the two real BraTS data sets (HG, LG) which indicates the results for three regions: complete tumor, tumor core, and reported Dice and Jaccard.

Table 1. Comparison results in real HG.

| Approach | Dice Complete tumor | Dice Tumor core | Dice Enhancing tumor | Jaccard Complete tumor | Jaccard Tumor core | Jaccard Enhancing tumor |
|---|---|---|---|---|---|---|
| Proposed method | 0.8377±0.105 | 0.759±0.15 | 0.761±0.19 | 0.733±0.14 | 0.635±0.19 | 0.647±0.21 |
| Meier et al. | 0.802±0.124 | 0.691±0.220 | 0.698±0.247 | 0.684±0.153 | 0.561±0.212 | 0.578±0.232 |
| Cordier et al. | 0.79±0.17 | 0.60±0.26 | 0.59±0.25 | - | - | - |
| Festa et al. | 0.83±0.08 | 0.7±0.24 | 0.75±0.16 | 0.72±0.12 | 0.58±0.25 | 0.63±0.18 |

Table 2. Comparison results in real LG.

| Approach | Dice Complete tumor | Dice Tumor core | Dice Enhancing tumor | Jaccard Complete tumor | Jaccard Tumor core | Jaccard Enhancing tumor |
|---|---|---|---|---|---|---|
| Proposed method | 0.792±0.11 | 0.652±0.08 | 0.44±0.26 | 0.66±0.14 | 0.503±0.12 | 0.33±0.24 |
| Meier et al. | 0.764±0.105 | 0.585±0.229 | 0.201±0.326 | 0.628±0.121 | 0.446±0.228 | 0.152±0.150 |
| Nicolas et al. | 0.76±0.18 | 0.64±0.21 | 0.44±0.4 | - | - | - |
| Festa et al. | 0.72±0.17 | 0.47±0.23 | 0.21±0.35 | 0.58±0.19 | 0.33±0.19 | 0.17±0.28 |

Fig. 11. Evaluation for the two synthetic BraTS data sets (HG, LG) which indicates the results for complete tumor.

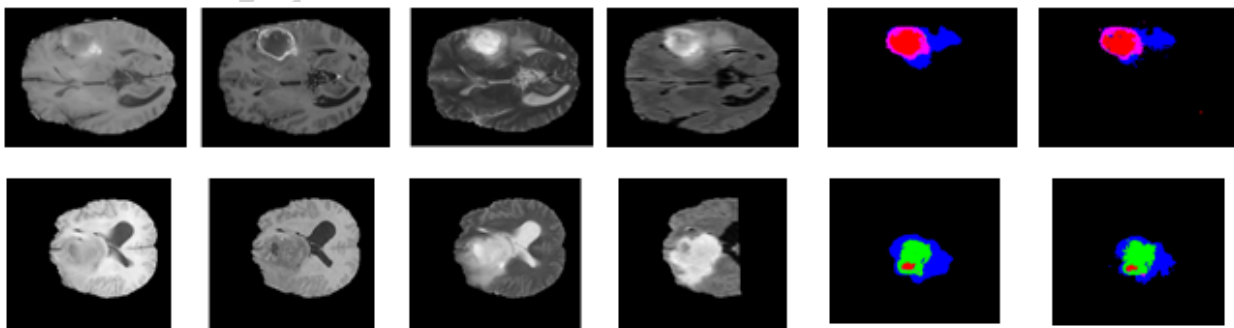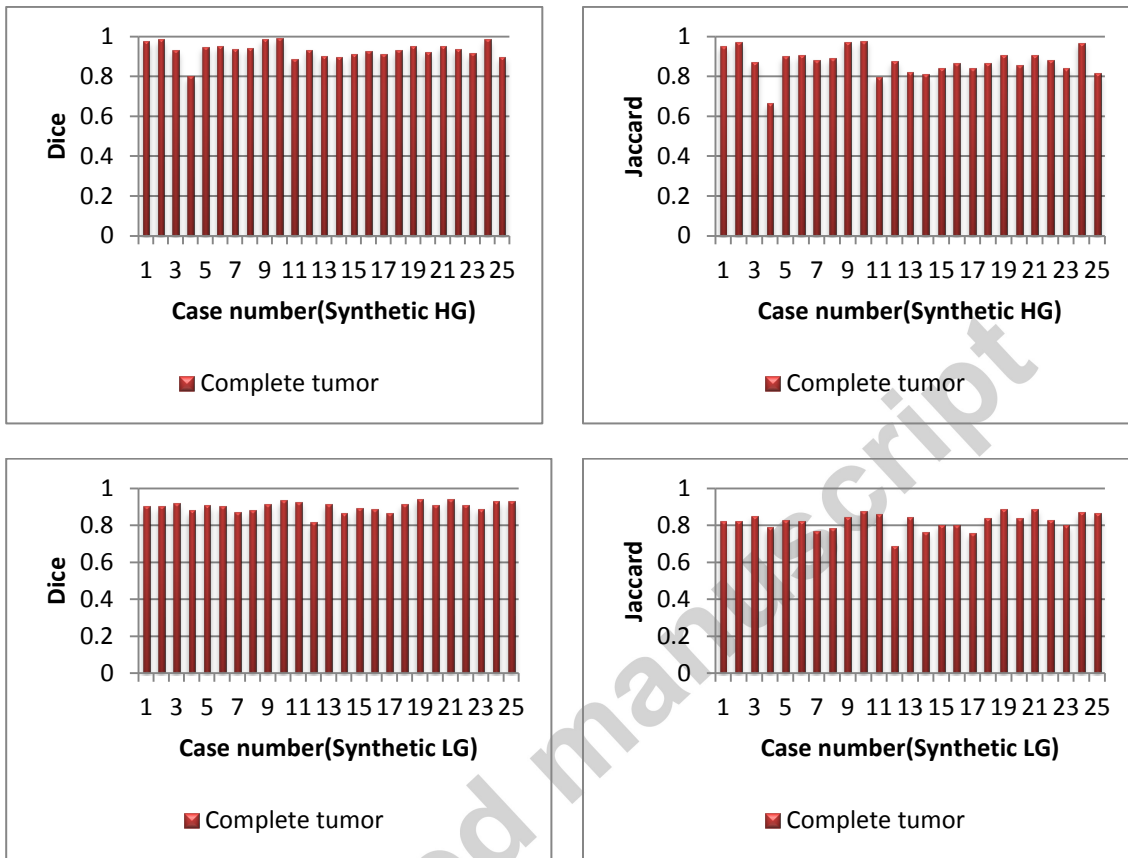Fig. 12. Segmented tissues with corresponding input and ground-truth images. Each row represents example set of multimodality MRI slices(first row is HG and second row is LG). ; Input: (a) T1, (b) T2,     (c) T1contrast (d) Flair. (e) ground-truth (f) Segmented image. Labels in the ground-truth: red-necrosis, blue- edema, green-non-enhancing tumor, magenta- enhancing tumor, black-everything else.

Table 3. Comparison results in synthetic data sets of HG and LG.

| Approach | Dice Complete Tumor(HG) | Jaccard Complete Tumor(HG) | Dice Complete Tumor(LG) | Jaccard Complete Tumor(LG) |
|---|---|---|---|---|
| Proposed method | 0.93±0.04 | 0.87±0.06 | 0.90±0.02 | 0.82±0.04 |
| Cordier et al. | 0.84±0.08 | - | 0.83±0.4 | - |

Table 4. Comparison results with BraTumIA software in real HG.

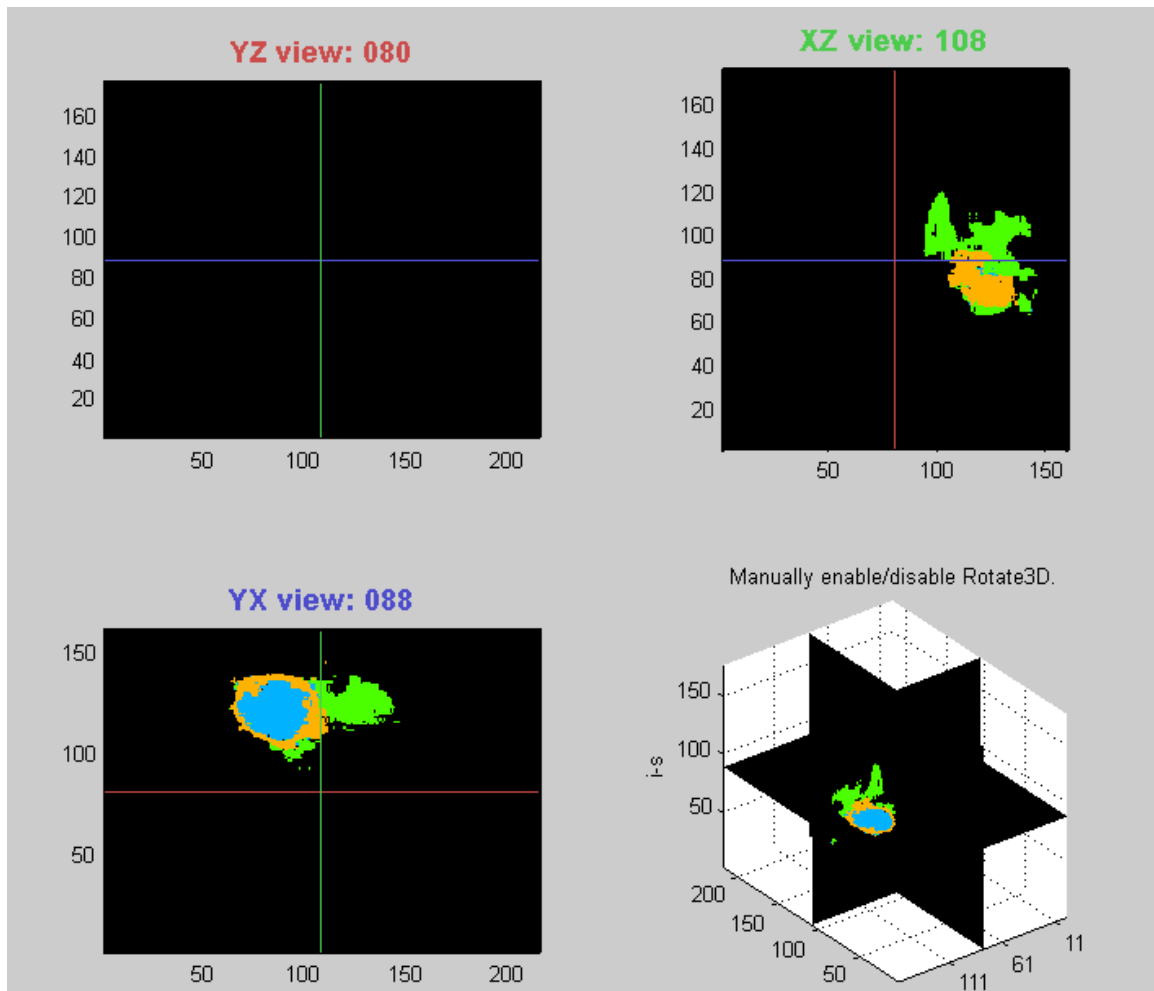| Approach | Dice Complete tumor | Dice Tumor core | Dice Enhancing tumor | Jaccard Complete tumor | Jaccard Tumor core | Jaccard Enhancing tumor |
|---|---|---|---|---|---|---|
| Proposed method | 0.8377±0.105 | 0.759±0.15 | 0.761±0.19 | 0.733±0.14 | 0.635±0.19 | 0.647±0.21 |
| BraTumIA software | 0.8178±0.068 | 0.692±0.195 | 0.709±0.21 | 0.696±0.094 | 0.554±0.18 | 0.58±0.20 |

Fig. 13. Three dimensional presentation of result, blue-necrosis, green- edema, red-non-enhancing tumor, orange-
enhancing tumor, black-everything else.

## 5. Conclusion and Future Work

In this paper we proposed a framework to segment tumorous MRI images. In the first step bias field correction is used to increase the contrast of the input image. Then histogram matching is used. In the second step, in order to reduce the time and space complexity especially in the feature extraction phase of the algorithm, the multi-level Otsu thresholding algorithm is used. Given to the large number of data in 3D imaging, using multi-level Otsu algorithm reduces the volume of the data. These images are imbalanced; applying this clustering algorithm selects more balanced distribution of data for training.

The third step, the feature extraction step, the local binary patterns (LBP-TOP) in three orthogonal planes and extended histogram of orientation gradients for 3D images (HOG-TOP) are used. The advantage of these features besides their simplicity is that they have a great discrimination capability for tissue images.

Finally, the random forest, which has a high accuracy in segmentation and can function perfectly with large inputs, is used as a classifier to distinguish tumorous regions. Our experimental evaluations indicate significantly better improvements in segmenting tumor images and reduction in time complexity. In our future work, we plan to study the performance of our algorithm on BRATS 2014 dataset.

References

[1]  S. Wang, M. Chen, Y. Li, Y. Zhang, L. Han, J. Wu, et al., Detection of dendritic spines using wavelet-based conditional symmetric analysis and regularized morphological shared-weight neural networks, Computational and Mathematical Methods in Medicine. 2015 (2015).

[2]  Y. Zhang, S. Wang, Detection of Alzheimer's disease by displacement field and machine learning, PeerJ. 3 (2015) e1251.

[3]  A.H. Gondal, M.N.A. Khan, A Review of Fully Automated Techniques for Brain Tumor Detection From MR Images, International Journal of Modern Education and Computer Science. 5 (2013) 55–61. doi:10.5815/ijmecs.2013.02.08.

[4]  A. von Deimling, Gliomas, Springer, 2009.

[5]  L.M. DeAngelis, Brain tumors, New England Journal of Medicine. 344 (2001) 114–123.

[6]  Z.-P. Liang, P.C. Lauterbur, Principles of magnetic resonance imaging, SPIE Optical Engineering Press, 2000.

[7]  S. Bauer, R. Wiest, L.-P. Nolte, M. Reyes, A survey of MRI-based medical image analysis for brain tumor studies, Physics in Medicine and Biology. 58 (2013) R97–R129. doi:10.1088/0031-9155/58/13/R97.

[8]  K. Popuri, D. Cobzas, A. Murtha, M. Jägersand, 3D variational brain tumor segmentation using Dirichlet priors on a clustered feature set, International Journal of Computer Assisted Radiology and Surgery. 7 (2012) 493–506. doi:10.1007/s11548-011-0649-2.

[9]  H. Cai, R. Verma, Y. Ou, S. Lee, E. Melhem, C. Davatzikos, Probabilistic segmentation of brain tumors based on multi-modality magnetic resonance images, 2007 4th IEEE International Symposium on Biomedical Imaging: From Nano to Macro. (2007) 600–603. doi:10.1109/ISBI.2007.356923.

[10]  R. Verma, E.I. Zacharaki, Y. Ou, H. Cai, S. Chawla, S.-K. Lee, et al., Multiparametric tissue characterization of brain neoplasms and their recurrence using pattern classification of MR images, Academic Radiology. 15 (2008) 966–977.

[11]  D. Geii, R. De Québec, T. France, U.D.R. Magnétique, C.H.U. De Caen, C. France, Tumor Segmentation From a Multispectral Mri Images By Using, 2 (2007) 1236–1239. doi:10.1109/ISBI.2007.357082.

[12]  S. Ruan, N. Zhang, Q. Liao, Y. Zhu, Image fusion for following-up brain tumor evolution, Proceedings - International Symposium on Biomedical Imaging. 3 (2011) 281–284. doi:10.1109/ISBI.2011.5872406.

[13]  T.R. Jensen, K.M. Schmainda, Computer-aided detection of brain tumor invasion using multiparametric MRI, Journal of Magnetic Resonance Imaging. 30 (2009) 481–489.

[14]  S. Wang, Y. Zhang, Z. Dong, S. Du, G. Ji, J. Yan, et al., Feed-forward neural network optimized by hybridization of PSO and ABC for abnormal brain detection, International Journal of Imaging Systems and Technology. 25 (2015) 153–164.

[15]  a Criminisi, J. Shotton, E. Konukoglu, Decision Forests for Classification , Regression , Density Estimation , Manifold Learning and Semi-Supervised Learning, Learning. 7 (2011) 81–227. doi:10.1561/0600000035.

[16]  E. Geremia, B.H. Menze, M. Prastawa, M. a. Weber, A. Criminisi, N. Ayache, Brain Tumor Cell Density

Estimation from Multi-modal MR Images Based on a Synthetic Tumor Growth Model, Medical Computer Vision Recognition Techniques and Applications in Medical Imaging. 7766 (2013) 273–282.

[17] H. Khotanlou, O. Colliot, I. Bloch, Automatic Brain Tumor Segmentation Using Symmetry Analysis and Deformable Models, Advances in Pattern Recognition - Proceedings of the Sixth International Conference. (2007) 198–202. doi:10.1142/9789812772381_0032.

[18] K.P. Remamany, T. Chelliah, K. Chandrasekaran, K. Subramanian, Brain Tumor Segmentation in MRI Images Using Integrated Modified PSO-Fuzzy Approach., International Arab Journal of Information Technology (IAJIT). 12 (2015).

[19] M. Agn, O. Puonti, P.M. af Rosenschöld, I. Law, K. Van Leemput, Brain Tumor Segmentation Using a Generative Model with an RBM Prior on Tumor Shape, in: Brainlesion: Glioma, Multiple Sclerosis, Stroke and Traumatic Brain Injuries, Springer, 2015: pp. 168–180.

[20] T. Wang, I. Cheng, A. Basu, Fluid vector flow and applications in brain tumor segmentation, Biomedical Engineering, IEEE Transactions on. 56 (2009) 781–789.

[21] J. Sachdeva, V. Kumar, I. Gupta, N. Khandelwal, C.K. Ahuja, A novel content-based active contour model for brain tumor segmentation, Magnetic Resonance Imaging. 30 (2012) 694–715.

[22] S. Ho, L. Bullitt, G. Gerig, Level-set evolution with region competition: automatic 3-D segmentation of brain tumors, in: Pattern Recognition, 2002 Proceedings 16th International Conference on, 2002: pp. 532–535.

[23] J. Rexilius, H.K. Hahn, J. Klein, M.G. Lentschig, H.-O. Peitgen, Multispectral brain tumor segmentation based on histogram model adaptation, in: Medical Imaging, 2007: p. 65140V–65140V.

[24] A. Pinto, S. Pereira, H. Dinis, C.A. Silva, D.M.L.D. Rasteiro, Random decision forests for automatic brain tumor segmentation on multi-modal MRI images, in: Bioengineering (ENBENG), 2015 IEEE 4th Portuguese Meeting on, 2015: pp. 1–5.

[25] S. Reza, K.M. Iftekharuddin, Multi-fractal texture features for brain tumor and edema segmentation, in: SPIE Medical Imaging, 2014: p. 903503.

[26] M. Kumar, K.K. Mehta, A Texture based Tumor detection and automatic Segmentation using Seeded Region Growing Method, 2 (2011) 855–859.

[27] V. Harati, R. Khayati, A. Farzan, Fully automated tumor segmentation based on improved fuzzy connectedness algorithm in brain MR images, Computers in Biology and Medicine. 41 (2011) 483–492.

[28] L.R. Schad, S. Blüml, I. Zuna, IX. MR tissue characterization of intracranial tumors by means of texture analysis, Magnetic Resonance Imaging. 11 (1993) 889–896.

[29] M.C. Clark, L.O. Hall, D.B. Goldgof, R. Velthuizen, F.R. Murtagh, M.S. Silbiger, Automatic tumor segmentation using knowledge-based techniques, Medical Imaging, IEEE Transactions on. 17 (1998) 187–201.

[30] N. Menon, R. Ramakrishnan, Brain Tumor Segmentation in MRI images using unsupervised Artificial Bee Colony algorithm and FCM clustering, in: Communications and Signal Processing (ICCSP), 2015 International Conference on, 2015: pp. 6–9.

[31] L.M. Fletcher-Heath, L.O. Hall, D.B. Goldgof, F.R. Murtagh, Automatic segmentation of non-enhancing brain tumors in magnetic resonance images, Artificial Intelligence in Medicine. 21 (2001) 43–63.

[32] D.-Y. Huang, T.-W. Lin, W.-C. Hu, Automatic multilevel thresholding based on two-stage Otsu's method with cluster determination by valley estimation, ICIC International Journal of Innovative Computing, Information and Control. 7 (2011) 5631–5644.

[33] I. Diaz, P. Boulanger, R. Greiner, A. Murtha, A critical review of the effects of de-noising algorithms on MRI brain tumor segmentation., Conference Proceedings : Annual International Conference of the IEEE Engineering in Medicine and Biology Society IEEE Engineering in Medicine and Biology Society Conference. 2011 (2011) 3934–7. doi:10.1109/IEMBS.2011.6090977.

[34] N.J. Tustison, B.B. Avants, P. Cook, Y. Zheng, A. Egan, P. Yushkevich, et al., N4ITK: improved N3 bias correction, Medical Imaging, IEEE Transactions on. 29 (2010) 1310–1320.

[35] T.S. Yoo, M.J. Ackerman, W.E. Lorensen, W. Schroeder, V. Chalana, S. Aylward, et al., Engineering and algorithm design for an image processing Api: a technical report on ITK--the Insight Toolkit., Studies in Health Technology and Informatics. 85 (2002) 586–592. doi:10.3233/978-1-60750-929-5-586.

[36] N. Otsu, A threshold selection method from gray-level histograms, Automatica. 11 (1975) 23–27.

[37] M. Sezgin, others, Survey over image thresholding techniques and quantitative performance evaluation, Journal of Electronic Imaging. 13 (2004) 146–168.

[38] A. Kassner, R.E. Thornhill, Texture analysis: a review of neurologic MR imaging applications, American Journal of Neuroradiology. 31 (2010) 809–816.

[39]    S. Ahmed, K.M. Iftekharuddin, A. Vossough, Efficacy of texture, shape, and intensity feature fusion for posterior-fossa tumor segmentation in MRI, Information Technology in Biomedicine, IEEE Transactions on. 15 (2011) 206–213.

[40]    M. Tuceryan, A.K. Jain, Texture Analysis Handbook of Pattern Recognition and Computer Vision: 207-248, (1998).

[41]    F. Tajeripour, E. Kabir, A. Sheikhi, Fabric Defect Detection Using Modified Local Binary Patterns, EURASIP Journal on Advances in Signal Processing. 2008 (2008) 783898. doi:10.1155/2008/783898.

[42]    T. Ojala, M. Pietikäinen, T. Mäenpää, Multiresolution gray-scale and rotation invariant texture classification with local binary patterns, Pattern Analysis and Machine Intelligence, IEEE Transactions on. 24 (2002) 971–987.

[43]    T. Ojala, M. Pietikäinen, D. Harwood, A comparative study of texture measures with classification based on featured distributions, Pattern Recognition. 29 (1996) 51–59.

[44]    G. Zhao, M. Pietikäinen, Dynamic texture recognition using local binary patterns with an application to facial expressions., IEEE Trans Pattern Analysis and Machine Intelligence. 29 (2007) 915–928. doi:10.1109/TPAMI.2007.1110.

[45]    D.G. Lowe, Distinctive image features from scale-invariant keypoints, International Journal of Computer Vision. 60 (2004) 91–110.

[46]    N. Dalal, B. Triggs, Histograms of Oriented Gradients for Human Detection, CVPR "05: Proceedings of the 2005 IEEE Computer Society Conference on Computer Vision and Pattern Recognition (CVPR"05) - Volume 1. (2005) 886–893. doi:10.1109/CVPR.2005.177.

[47]    L. (University of C. Breiman, Random forest, Machine Learning. 45 (1999) 1–35. doi:10.1023/A:1010933404324.

[48]    T.G. Dietterich, Ensemble Methods in Machine Learning, Multiple Classifier Systems. (1990) 1–15. doi:10.1007/3-540-45014-9_1.

[49]    T. Sørensen, {A method of establishing groups of equal amplitude in plant sociology based on similarity of species and its application to analyses of the vegetation on Danish commons}, Biol Skr. 5 (1948) 1–34.

[50]    P. Jaccard, Distribution de la Flore Alpine: dans le Bassin des dranses et dans quelques r{é}gions voisines, Rouge, 1901.

[51]    B.H. Menze, A. Jakab, S. Bauer, J. Kalpathy-Cramer, K. Farahani, J. Kirby, et al., The multimodal brain tumor image segmentation benchmark (BRATS), IEEE Transactions on Medical Imaging. 34 (2015) 1993–2024.

[52]    R. Meier, S. Bauer, J. Slotboom, R. Wiest, M. Reyes, A hybrid model for multimodal brain tumor segmentation, Multimodal Brain Tumor Segmentation. (2013) 31.

[53]    N. Cordier, B. Menze, N. Ayache, N. Cordier, B. Menze, N.A.P. Segmen-, et al., Patch-based Segmentation of Brain Tissues To cite this version : Patch-based Segmentation of Brain Tissues, (2013).

[54]    J. Festa, S. Pereira, J.A. Mariz, N. Sousa, C.A. Silva, Automatic brain tumor segmentation of multi-sequence mr images using random decision forests, Proceedings of NCI-MICCAI BRATS. 1 (2013) 23–26.

[55]    N. Porz, S. Bauer, A. Pica, P. Schucht, J. Beck, R.K. Verma, et al., Multi-modal glioblastoma segmentation: man versus machine, (2014).

Solmaz Abbasi received her B.Sc. degree in Computer Engineering from Shiraz Payamnoor University, Shiraz, Iran, in 2010, and her M.Sc. degree in Artificial Intelligence from Shiraz University, Iran, in 2015. Her research interests include texture classification, pattern recognition, computer vision and video processing.



Farshad Tajeripour received his B.Sc. and M.Sc. degrees in Electronic Engineering from Shiraz University, Shiraz, Iran, in 1994 and 1997. He received Ph.D. degree in Electronic Engineering from Tarbiat Modarres, Tehran, Iran, in 2009. Currently he is an assistant professor in Shiraz University. His research interests include texture classification, pattern recognition, computer vision and video processing.